Preliminary Diffusive Clearance of Silicon Nanopore Membranes in a Parallel Plate Configuration for Renal Replacement Therapy

Steven Kim,*† James Heller,* Zohora Iqbal,* Rishi Kant,* Eun Jung Kim,* Jeremy Durack,‡§ Maythem Saeed,‡§ Loi Do,‡§ Steven Hetts,‡§ Mark Wilson,‡§ Paul Brakeman,¶ William H. Fissell,‖ and Shuvo Roy*

Silicon nanopore membranes (SNMs) with compact geometry and uniform pore size distribution have demonstrated a remarkable capacity for hemofiltration. These advantages could potentially be used for hemodialysis. Here, we present an initial evaluation of the SNM's mechanical robustness, diffusive clearance, and hemocompatibility in a parallel plate configuration. Mechanical robustness of the SNM was demonstrated by exposing membranes to high flows (200 ml/min) and pressures (1,448 mm Hg). Diffusive clearance was performed in an albumin solution and whole blood with blood and dialysate flow rates of 25 ml/min. Hemocompatibility was evaluated using scanning electron microscopy and immunohistochemistry after 4 hours in an extracorporeal porcine model. The pressure drop across the flow cell was 4.6 mm Hg at 200 ml/min. Mechanical testing showed that SNM could withstand up to 775.7 mm Hg without fracture. Urea clearance did not show an appreciable decline in blood *versus* albumin solution. Extracorporeal studies showed blood was successfully driven *via* the arterial–venous pressure differential without thrombus formation. Bare silicon showed increased cell adhesion with a 4.1-fold increase and 1.8-fold increase over polyethylene glycol (PEG)–coated surfaces for tissue plasminogen factor (t-PA) and platelet adhesion (CD41), respectively. These initial results warrant further design and development of a fully scaled SNM-based parallel plate dialyzer for renal replacement therapy. *ASAIO Journal* 2016; 62:169–175.

Key Words: MEMS, microfabrication, portable hemodialysis, parallel plate dialyzer

End-stage renal disease (ESRD) remains a major public health problem in the United States—afflicting more than 615,000 people with nearly 116,000 new patients initiating treatment each year.[1] Because of the shortfall in organ availability, the majority of patients with ESRD in the United States must undergo in-center, 3–4 hours, thrice weekly hemodialysis. Currently, high-flux hollow-fiber dialyzers have usurped all other membrane technologies given their large surface area, favorable transport, and low manufacturing costs. However, polymer hollow-fiber membranes have several inherent limitations that hinder further advancements and have resulted in stagnant patient outcomes. First, significant blood-to-dialysate flow mismatch can occur because of uneven blood flow distribution and dialysate channeling from uneven fiber packing.[2] Second, polymer membranes have inherent biocompatibility problems because of clotting and activation of platelet, leukocyte, and complement, which limits long-term continuous use.[3] Third, the high internal resistance of hollow-fiber dialyzers requires an external blood pump that also results in deleterious cell activation and microbubble formation.[4] Finally, hollow-fiber polymer membranes have wide pore size distributions, tortuous flow paths, and roughly circular-shaped cross sectional pore geometries that limit their selectivity and permeability compared with slit-pore geometries.[5]

Parallel plate dialyzers, on the other hand, allow for the potential for uniform blood and dialysate flow across a flat surface. The internal flow resistance with a large width to height ratio is dependent on the viscosity, path length, blood flow rate, and width to height dimensions.[6] Therefore, by manipulating the height and width of the flat plate channel the internal resistance can be significantly reduced, negating the need for an external blood pump. These attributes popularized the flat plate hemodialyzer design,[7–10] and the Kiil dialyzer dominated the market in the 1960s.[11] However, because of deficiencies in membrane technology at the time and advantages of hollow-fiber membranes, the flat plate design was supplanted. Today, however, microelectromechanical systems (MEMSs) technology enables cost-effective production of flat sheets of silicon-based membranes with unprecedented control of pore size and geometry.[12] Therefore, there is increased interest in combining new and innovative silicon-based membrane technology with the advantageous design elements of the parallel plate dialyzer.

From the *Department of Bioengineering and Therapeutic Sciences, †Division of Nephrology, University of California San Francisco, San Francisco, California; ‡Department of Radiology and Biomedical Imaging, University of California San Francisco, San Francisco, California; §UCSF Imaging Center at China Basin, San Francisco, California; ¶Division of Pediatric Nephrology, University of California San Francisco, San Francisco, California; and ‖Division of Nephrology and Hypertension, Vanderbilt University Medical Center, Nashville, Tennessee.

Jeremy Durack is currently at Department of Radiology, Memorial Sloan Kettering Cancer Center, 1275 York Avenue, Suite H-118, New York, New York.

Submitted for consideration April 2015; accepted for publication in revised form October 2015.

Disclosure: This work was supported by the American Society of Nephrology Ben J. Lipps Research Fellowship, National Institute of Biomedical Imaging and Bioengineering of the National Institutes of Health under Award Number R01 EB014315, Wildwood Foundation, and the John and Marcia Goldman Foundation.

Supplemental digital content is available for this article. Direct URL citations appear in the printed text, and links to the digital files are provided in the HTML and PDF versions of this article on the journal's Web site (www.asaiojournal.com).

Correspondence: Steven Kim, MD, Division of Nephrology, University of California, 521 Parnassus Ave, San Francisco, California 94143. E-mail: steven.kim@uscf.edu.

DOI: 10.1097/MAT.0000000000000311

Recently, Ahmadi *et al.*[13] and Johnson *et al.*[14] used flat MEMS-based ultrathin porous nanocrystalline silicon membranes from SiMPore (West Henrietta, NY) to investigate *in vitro* clearance of small molecules and hemocompatibility using a single parallel plate configuration. These flat membranes had average circular pore sizes of 5 and 20 nm with a membrane thickness of 30 nm. They were able to show clearance of small solutes over a total membrane area of 3 mm^2. The main limitation was fragility of the membrane requiring testing at very low flow rates (82.5 µl/min) and static dialysate to avoid mechanical failure.

Our group has previously pioneered a novel and robust silicon nanopore membranes (SNMs) based on MEMS fabrication techniques for use in a fully implantable bioartificial kidney. The SNMs have been extensively evaluated for their ability to function as a hemofilter.[5,12,15] The slit-pore design allows for an order of magnitude higher hydraulic permeability than commercially available hollow-fiber membranes.[15] Furthermore, the uniform pore size of SNM allows for extremely selective size-based filtration with strict molecular weight cut-offs.

To exploit the advantages of a parallel plate design, we have investigated the ability of SNM to perform diffusive clearance. In this initial evaluation, we first examined the mechanical robustness of SNM under supraphysiologic conditions. Next, diffusive clearance of a scaled-down array of SNM in a parallel plate channel was tested. We compared transport in an albumin solution *versus* whole blood to evaluate any decline in membrane transport in a blood environment. Finally, we tested pumpless blood flow in an extracorporeal parallel plate circuit to assess thrombosis and surface cell adhesion. By characterizing key parameters necessary to evaluate a SNM-based parallel plate dialyzer, our intent is to lay the foundation for future large-scale devices.

Materials and Methods

Membrane Fabrications

Silicon nanopore membranes were fabricated using previously described microfabrication techniques.[12] Membranes were composed of a 300 nm polysilicon layer with an array of rectangular pore slits measuring 4.5 µm × 10 nm. The structural support layer was composed of <100> oriented, n-type crystalline silicon with 400 µm thickness. Wafers were diced into 10 × 10 mm chips with an effective membrane area of 0.216 cm^2. The hydraulic permeability of SNM was tested to verify membrane integrity and determine pore size.[12]

Surface Modification

Polyethylene glycol (PEG) surface modification was performed on polysilicon surfaces.[16] SNMs were treated with a 3:1 sulfuric acid to hydrogen peroxide (Piranha, Avantor Performance Materials, Center Valley, PA) solution to functionalize the polysilicon surface with hydroxyl groups. Membranes were submersed in 25 ml of toluene and 285 µl of PEG-silane (Sigma Aldrich, St. Louis, MO) at 70°C for 2 hours. Surface modified membranes were then rinsed at 10 minutes intervals (3×) with toluene (Gelest Morrisville, PA), ethanol, and deionized water. Hydraulic permeability was retested after PEG coating to measure the pore size change after surface modification. SNM coating thickness was sub-5 nm.

Parallel Plate Array Flow Cell

A two-channel parallel plate flow cell capable of housing and testing multiple SNM chips exposed to blood flow was developed (**Figure 1**). It consisted of two titanium (grade 2 commercially pure) inlet and outlet ports. These were positioned perpendicular to the plates for even fluid distribution. The main body of the device consisted of a stacked set of parallel plates (titanium, grade 2 commercially pure), with alternating channels for blood (internal part of each plate) and dialysate flow (in the interfaces between the plates). A single internal blood channel was 60 mm × 30 mm × 2.4 mm ($l \times w \times h$) and defined by a top plate (solid silicon sheet, 6 × 3 cm) and bottom plate (eight SNMs or solid silicon mounted into the titanium holder with polydimethylsiloxane). The plates

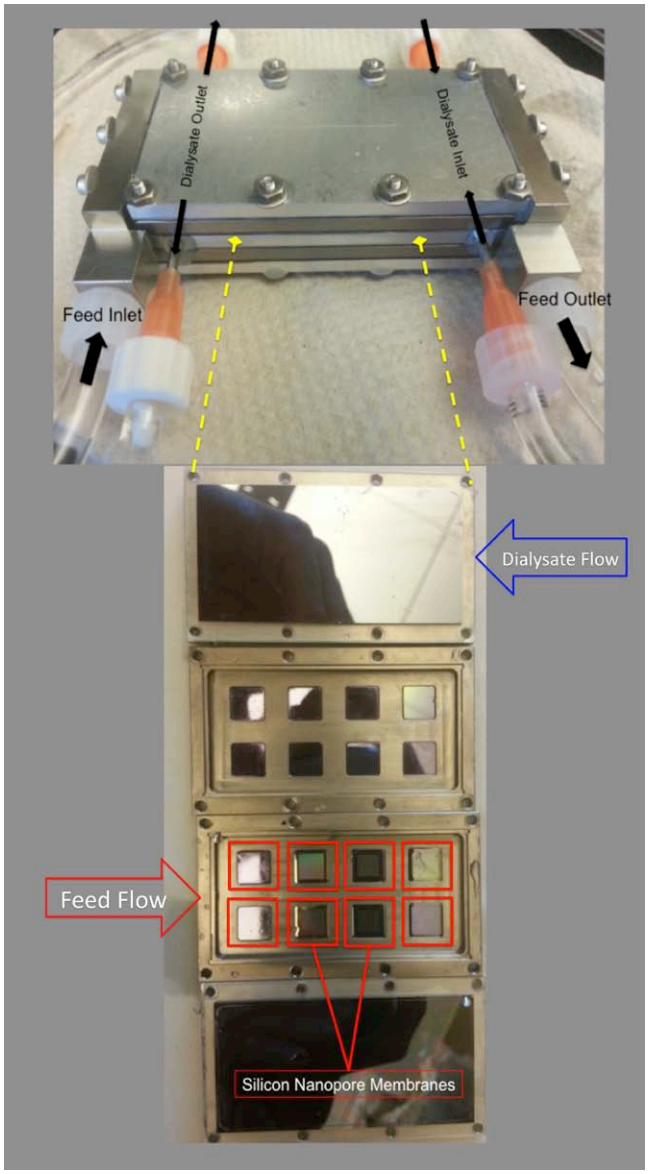

Figure 1. Assembled parallel plate array with blood inlet/outlet and counter-current dialysate inlet/outlet. The stacked parallel plates are shown below with eight silicon nanopore membranes outlined in red and eight solid silicon chips (not outlined). The arrows indicate the flow inlet and direction of the feed and dialysate, respectively. full color online

were sealed together using high purity silicone gaskets and screws to prevent leakage. Dialysate flow was split into two inlet ports and two outlet ports on the center plate. Uniform dialysate flow in a counter-current direction was achieved *via* an array of multiple 1 mm diameter channels across the width of the dialysate plate. The dialysate channel was defined by the height of the compressed gasket (0.4 mm) with length of 60 mm and width of 30 mm. The titanium-end caps were machined by Hayes Manufacturing Services (Sunnyvale, CA) and the remaining components were machined in our laboratory. SolidWorks software (DS Solidworks, Waltham, MA) was used to design all components.

Mechanical Testing

Mechanical robustness of SNM was tested at a range of pressures (1,448 mm Hg) using a syringe pump (KD410, KDS Scientific, Holliston, MA) and pressure gauge (DPI 104 30 psi, GE Druck, Leicester, United Kingdom). Pressure was ramped at 25.9 mm Hg until membrane rupture or 1448 mm Hg was reached (n = 11).

Static and dynamic leak testing of the parallel plate array was conducted over a range of differential pressures (0–200 mm Hg). Pressure drop across the array (inlet to outlet) was measured over a range of flow rates (0–200 ml/min). A Masterflex L/S Digital Drive Peristaltic Pump (MK-07551-00, Cole Parmer, Vernon Hills, IL) was used to drive flow, and pressure in the system was monitored using two pressure gauges (DPI 104 10 psi, GE Druck).

Parallel Plate Array Diffusive Clearance

Eight PEG-coated SNM chips were mounted onto the blood channel plate of the flow cell. The average pore size of the SNM was 6.5 ± 0.6 nm, and the combined effective membrane surface area was 1.73 cm^2. The albumin solution consisted of creatinine 10 mg/dl (Acros Organics, Geel, Belgium), 88 mg/dl blood urea nitrogen (Fisher Scientific, Waltham, MA), 5 mg/dl phosphorus (Sigma, St. Louis, MO), and 3 g/dl albumin (Sigma) in Millipore water (Millipore, Billerica, MA) in a volume of 13 ml. Whole blood diffusion experiments were conducted using 30 ml of heparinized (20 units/ml) bovine whole blood (Lampire Biological Laboratories, Pipersville, PA). The albumin solution or whole blood was recirculated and 1 L of dialysate (140 mEq of NaCl) was recirculated in a counter-current fashion (**Figure 1**). The flow rates for both solutions were set to 25 ml/min using a peristaltic pump to maintain pressures of <30 mm Hg and limit transmembrane pressures. The system was preconditioned with the solutions for 30 minutes. Samples of albumin solution or whole blood and dialysate were collected at 0, 2, and 5 hours (n = 3). The whole blood experiments were also conducted for 24 hours (n = 2). The flow cell was disassembled and evaluated for thrombus formation, membrane fracture, or leaks. The concentrations of the different solutes were measured using an Avida 1800 Chemistry System (Siemens Medical, Erlangen, Germany) at San Francisco General Hospital (San Francisco, CA). Solute clearance (K) was calculated by fitting concentrations measured at serial time points an exponential decay function: $C(t) = C_i e^{-Kt/V}$, where $C(t)$ was the concentration at time t, C_i was the initial concentration, t was the time, and V was the volume.

Extracorporeal Porcine Experiment

Pumpless blood flow characteristic in a parallel plate SNM array within an extracorporeal blood circuit was evaluated in a pig for 4 hours with University of California, San Francisco Institutional Animal Care and Use Committee approval. A ~20 kg Yorkshire pig was anesthetized and systematic heparin anticoagulation therapy was delivered in bolus (200 IU/kg) followed by continuous infusion (125 IU/kg/hour). The renal artery and vein were cannulated using ultrasound and fluoroscopic guidance, with two single-lumen catheters (Deltec Ventra Long-term Central Venous Catheters, Single-Lumen, 9FR, PN 21-2368-01, Smiths Medical, Dublin, OH). The inlet of the flow cell was attached to the arterial catheter and outlet was attached to the venous catheter, completing the extracorporeal arteriovenous circuit. Several minutes after the experiment began, a fluoroscopic contrast agent (Omnipaque 300, GE Healthcare, Little Chalfont, United Kingdom) was injected. Cine images were obtained during a 90 second dynamic infusion of contrast. Gross qualitative flow through the device was evaluated.[17]

The extracorporeal circuit was run for a total of 4 hours uninterrupted. At the end of the experiment, with the device still attached, a second bolus of contrast agent was delivered and the device was reimaged. The contrast front was again visualized flowing across the device. The arterial and venous catheters were then clamped, and the device was disconnected from the extracorporeal circuit and drained. To prevent the remaining stagnant blood from coagulating, the cartridge was immediately cleared with heparinized saline until it ran clear. It was fully drained and then primed with a solution of 4% paraformaldehyde and deionized water. The device was carefully disassembled to examine the device for thrombus formation and leakage (see Figures S1 and S2, Supplemental Digital Contents 1 and 2, http://links.lww.com/ASAIO/A80 and http://links.lww.com/ASAIO/A81).

Cell and Protein Adhesion Studies

Scanning Electron Microscopy. The SNM were placed in a solution containing 2% glutaraldehyde (Electron Microscopy Sciences, Fort Washington, PA), 3% sucrose (Sigma Aldrich) and 0.1 M of phosphate buffered saline (PBS) at 4°C and pH 7.4. After 1 hour, the substrates were rinsed twice with PBS for 30 minutes at 4°C and washed with distilled water for 5 minutes. Dehydration was achieved by placing the substrates in 50% ethanol for 15 minutes while increasing the concentration of ethanol to 60%, 70%, 80%, 90%, and finally 100%. Dehydrated samples were then mounted on aluminum stubs, sputter-coated with gold–palladium, and examined using Scanning Electron Microscopy (SEM; Ultra55 FEGSEM, ZEISS, Peabody, MA).

Immunohistochemistry. Platelet adhesion and activation was assessed using immunofluorescence staining for the platelet marker, CD41 (Abcam, Cambridge, MA), and blood-clot marker, tissue plasminogen activator (t-PA, Abcam, Cambridge, MA). Platelets were fixed in 4% paraformaldehyde (Fisher Scientific, Waltham, MA) for 15 minutes followed by incubation in 1% bovine serum albumin for 30 minutes to block nonspecific binding. Platelets were double-labeled as follows: substrates were first incubated

with primary antibodies (t-PA), diluted 1:50 in PBS for 60 minutes followed by Alexa Fluor 546 donkey anti-mouse antibody (Invitrogen, Carlsbad, CA) diluted 1:100 in PBS for 60 minutes. Finally, the samples were incubated with anti-human CD41 fluorescein isothiocyanate labeled mouse monoclonal antibody diluted 1:300 in PBS for 60 minutes. Four images were acquired per replicate using a Nikon Eclipse Ti-E motorized inverted microscope (Nikon Instruments Inc., Melville, NY) to obtain a total of 12 images per substrate. The fluorescent intensity of the images was quantified using ImageJ.[18–20]

Results

Mechanical Testing

All SNMs withstood mechanical pressure testing greater than 775.7 mm Hg. Four out of 11 SNMs failed with an average pressure of 910.2 ± 51.7 mm Hg, and the remaining seven SNMs remained intact up to 1,448 mm Hg. The parallel plate array was tested at varying flow rates up to 200 ml/min without leakage of fluid out of the assembled device or between the individual parallel plates. The measured pressure drop across the flow cell at a flow rate of 200 ml/min was 4.6 mm Hg (see Figures S3 and S4, Supplemental Digital Contents 3 and 4, http://links.lww.com/ASAIO/A82 and http://links.lww.com/ASAIO/A83).

Diffusive Clearance of SNM Parallel Plate Array

The change in concentration using single-pass measurements was below the level of detection because of the high flow rate indicating that diffusive clearance was no longer dependent on flow rate. Recirculated albumin solution and whole blood concentrations of creatinine, urea, and phosphorus followed an exponential decay function characteristic of diffusive clearance. The clearance (*K*) normalized to SNM surface area for albumin solution and whole blood experiments are shown in **Table 1**. The initial albumin concentration was 3.17 ± 0.05 g/dl and 5 hour albumin concentration was 3.13 ± 0.12 g/dl. There was no significant reduction in albumin concentration ($p < 0.05$). Overall, heparinized bovine whole blood experiments showed maintenance of diffusive clearance similar to albumin solution. There was no evidence of clot formation during the 2 and 5 hour collection times. However, there was visible clot formation within the blood reservoir after 24 hours. Upon disassembly of the device, it was found there were no gross thrombi or membrane occlusion after 24 hours of continuous blood circulation.

Table 1. Clearance (*K*) for Creatinine, Urea, and Phosphorus in Albumin Solution and Whole Blood

	Diffusive Clearance (ml/min/m^2)	
	Parallel Plate Array (Albumin Solution)	Parallel Plate Array (Whole Blood)
Creatinine	84.0 ± 15.3	127.6 ± 14.0
Urea	115.2 ± 17.8	117.1 ± 16.0
PO_4	64.2 ± 14.7	56.5 ± 9.6

Porcine Extracorporeal Circuit

The preliminary extracorporeal circuit study demonstrated pumpless blood flow through the parallel plate array without complications. The pig tolerated the device well and did not exhibit deterioration of hemodynamic parameters or clinical

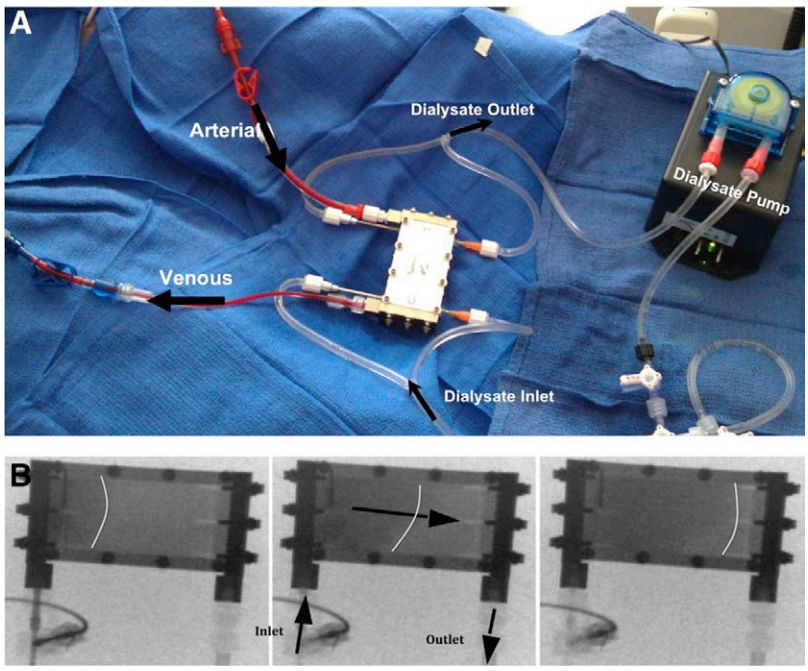

Figure 2. A: *Ex vivo* porcine experiment. Arterial and venous inlet and outlet labeled with arrows indicating the direction of flow. Dialysate inlet and outlet with arrows indicating the counter-current flow of dialysate. B: Fluoroscopy time-lapse images (top down view). Cine images were obtained after a 90 second dynamic infusion of contrast. Representative images at the start, middle, and end of contrast infusion are shown. White lines are labeled to indicate contrast front. Black arrows show direction for blood flow. full color online

status (**Figure 2A)**. The fluoroscopy images obtained at the start and end of the 4 hour experiment showed no degradation in flow characteristics, with uniform blood flow across the parallel plates (**Figure 2B)**. There was no evidence of thrombus formation in the cannulated vessels or catheter. Disassembly of the device showed no visible thrombi or debris within the flow cell.

Hemocompatibility Assessment

After disassembly of the flow cell, the silicon was imaged by SEM. There was cell adhesion on blood-exposed surfaces for both uncoated silicon and PEG-coated silicon. However, there was visually less platelet and neutrophil adhesion on the surface of PEG-coated silicon compared with bare silicon (**Figure 3**). Representative images showing platelet adhesion and blood clots were visualized by immunofluorescence staining for CD41 and t-PA on uncoated silicon and PEG-coated silicon surfaces (**Figure 4**). Total fluorescent intensity was used to quantify the amount of staining on the surface. Bare silicon surfaces had a 4.1-fold increase in fluorescent intensity for t-PA and a 1.8-fold increase in fluorescent intensity for CD41 compared with PEG-coated surfaces.

Discussion

As discussed previously, prior ultrathin silicon membranes have been limited because of their mechanical fragility.[13] Here, we demonstrated the mechanical robustness of SNM by showing that the membranes can consistently withstand pressures beyond 775.7 mm Hg, which is well beyond any physiologic pressure encountered clinically. Of note, four out of 11 membranes failed before reaching the system maximum 1448 mm Hg indicating mechanical differences at these extreme pressures. We also tested the SNM at flow rates as high as 200 ml/min. These results demonstrate that SNM are able to handle a broad range of flow rates and transmembrane pressure gradients without concern for membrane integrity.

SNMs within a parallel plate flow cell were able to dialyze small solutes, although maintaining selectivity for larger macromolecules. The clearance values are comparable with current commercial polymer hollow-fiber membranes at low blood flow rates (200 ml/min) when normalized to surface area (**Table 2**). This preliminary study also demonstrated the ability of the SNM parallel plate flow cell to function in a blood environment. The device was able to clear solutes in bovine whole blood for up

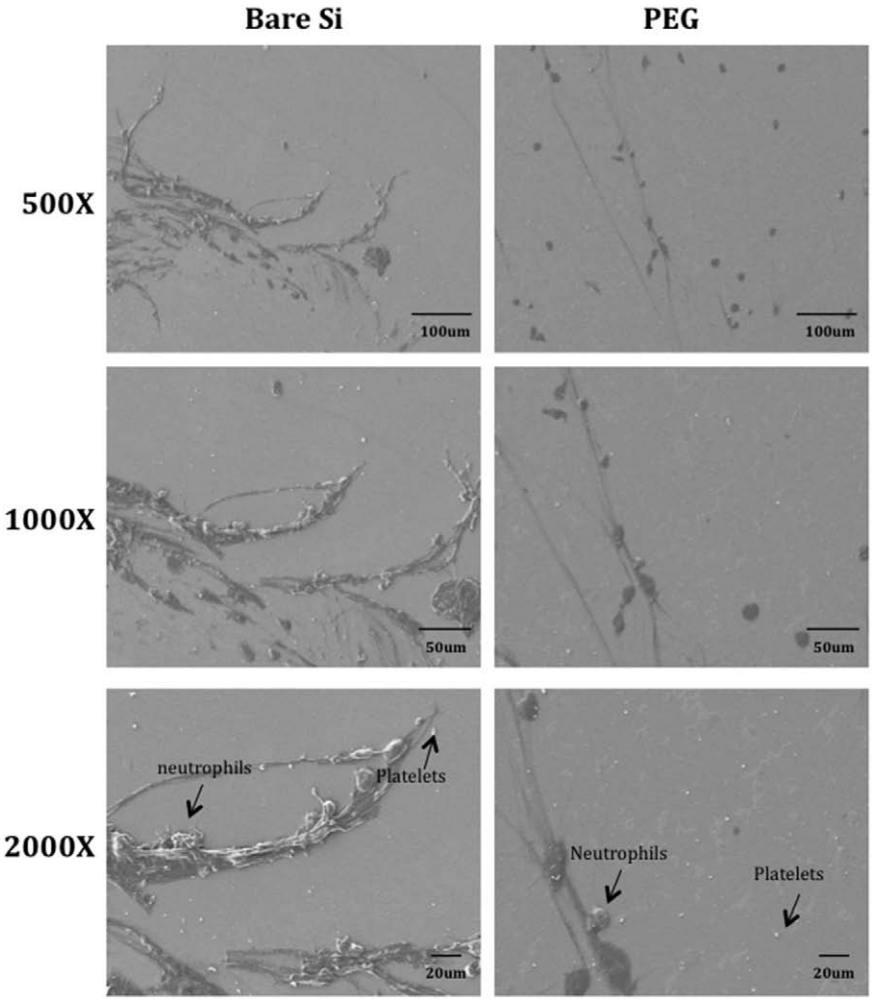

Figure 3. Scanning electron microscopy (SEM) images showing neutrophils (average sizes: 12–17 μm), platelets (average sizes: 1–6 μm), and red blood cells (average sizes: 8–10 μm) adhesion on bare silicon (Si) and polyethylene glycol-coated substrates. Thread-like structures represent fibrin formation.

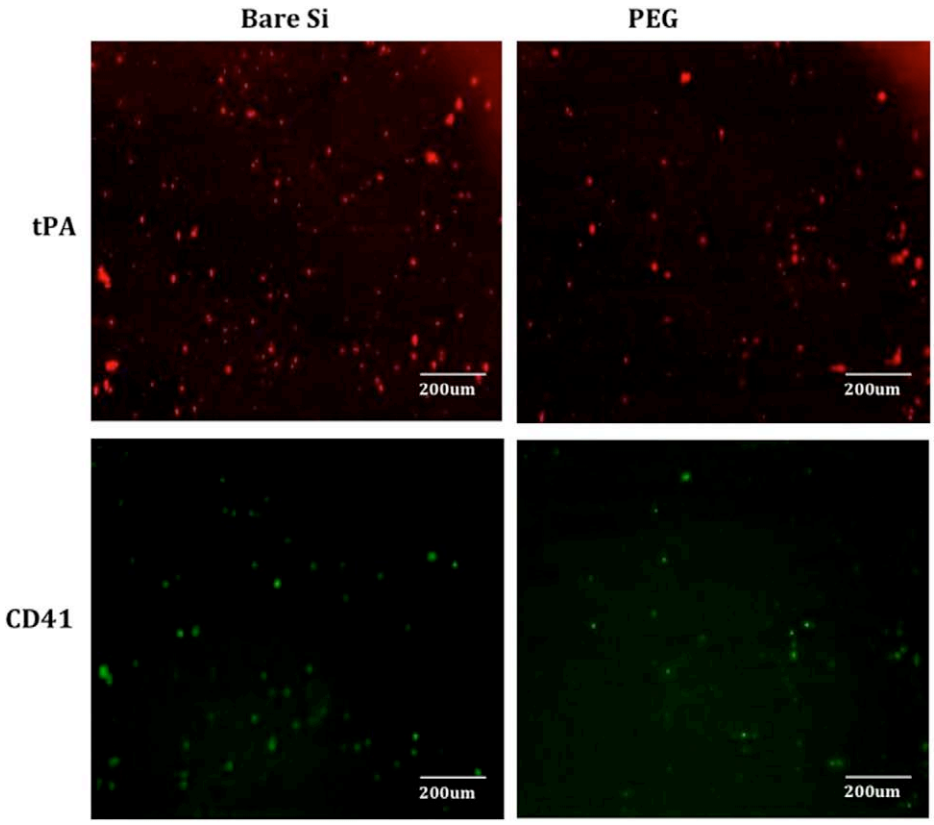

Figure 4. Representative images showing platelet adhesion and blood clots as visualized by immunofluorescence staining for t-PA (in red, blood clotting marker) and CD41 (in green, platelet marker) and on varying substrates after porcine study, bare silicon (Si) and PEG-coated substrates. full color online

to 24 hours without evidence of significant decline in diffusive transport. A potential wearable artificial kidney device that is used daily for 8 hours would require a minimum sp (single pool) *Kt/V* of 0.34 per treatment (V = 35 L) to achieve a weekly std (standard) *Kt/V* of 2.0.[21] Based on the presented clearance values for the SNM, we would require a total of 0.21 m^2 surface area. This would result in a device about the size of a coffee cup with approximately 25–30 stacked parallel plates each with 10 × 8 cm membrane area.

The extracorporeal study showed effective blood flow using only the arterial–venous pressure differential in a heparinzed pig without evidence of major thrombus after 4 hours. After disassembly, there was no evidence of visual clot formation within the flow cell or on the silicon surfaces. This indicates that during the 4 hour experiment, we had adequate blood flow characteristics to limit gross thrombosis. Surface analysis of the silicon showed also minimal platelet and clot formation; however, microemboli were not evaluated and could lead to embolic disease. Nevertheless, this animal study showed the feasibility of an extracorporeal pumpless parallel plate system using silicon substrates for short-term use. Furthermore, investigation is warranted for long-term studies especially looking at blood material interaction, flow optimization within a parallel plate system, and microemboli formation.

The sub-5 nm PEG-coated silicon showed significantly decreased cell and platelet adhesion compared with uncoated silicon. These thin-film coatings are a critical component to SNM feasibility for continuous long-term blood contact as they limit biofouling while still maintaining pore patency. Further work is being pursued with longer term studies as well as exploration of other polymer surface coatings with enhanced biocompatibility and stability.

The main barrier to improving diffusive transport of the SNM is the 400 μm membrane thickness, which is because of the standard silicon wafer thicknesses used to fabricate the SNM. In contrast, hollow-fiber membranes have thickness ranges of 40–50 μm. Our group is currently working to develop the next generation of SNM with significantly thinner membranes comparable with

Table 2. Urea Clearance (*K*) for Commercial Hollow-Fiber Dialyzers Normalized to Surface Area Clinical Blood Flow Rates (Q_b) and Dialysate Flow Rates (Q_d)

	Surface Area (m^2)	*K* (ml/min/m^2), Q_b = 200 ml/min, Q_d = 500 ml/min	*K* (ml/min/m^2), Q_b = 400 ml/min, Q_d = 500 ml/min
Fresenius Optiflux F160NR	1.5	129	205
Gambro Polyflux Revaclear	1.4	140	229
Asahi APS-650	1.3	143	210

commercial hollow-fiber membranes. This could theoretically increase the diffusive clearance of the membranes several fold and comparable with the mass transfer-area coefficient (KoA) of modern hollow-fiber dialyzers. However, reduction in the thickness of the membrane to improve diffusion must be weighed against the mechanical robustness of the membranes.

Conclusions

This study represents a preliminary evaluation of flat sheets of SNM for diffusive clearance in a parallel plate system. These promising results show that comparable diffusive clearance with hollow-fiber membranes is feasible in a compact device. We have also demonstrated diffusive transport that was not hindered by blood contact for 24 hours. Furthermore, we showed pumpless blood flow in an extracorporeal circuit without major thrombosis or significant surface fouling. However, significant challenges remain to translate these preliminary results into a fully scaled portable parallel plate hemodialyzer. Controlling blood and dialysate flow through multiple parallel plates without leaking are a nontrivial challenge. Blood flow optimization at the inlet and outlet, uniform flow across the parallel plates, vascular connections, and mechanical shock are additional challenges that will further complicate a fully scaled device. Nevertheless, the promising results justify further SNM optimization for diffusion, scaled parallel plate hemodialyzer design, and further extracorporeal blood compatibility studies.

Acknowledgment

The assistance of Charles Blaha, Illya Gordon, Torin Yeager, and Peter Soler on various aspects of experimentation and discussion are appreciated.

References

1. United States Renal Data System. 2015 USRDS annual data report: Epidemiology of kidney disease in the United States. National Institutes of Health, National Institute of Diabetes and Digestive and Kidney Diseases, Bethesda, MD, 2015.
2. Ronco C: Fluid mechanics and crossfiltration in hollow-fiber hemodialyzers. *Contrib Nephrol* 158: 34–49, 2007.
3. Takemoto Y, Naganuma T, Yoshimura R: Biocompatibility of the dialysis membrane. *Contrib Nephrol* 168: 139–145, 2011.
4. Daugirdas JT, Bernardo AA: Hemodialysis effect on platelet count and function and hemodialysis-associated thrombocytopenia. *Kidney Int* 82: 147–157, 2012.
5. Conlisk AT, Datta S, Fissell WH, Roy S: Biomolecular transport through hemofiltration membranes. *Ann Biomed Eng* 37: 722–736, 2009.
6. Hoenich N, Woffindin C, Ward M. Dialysers, in: Maher J (ed). *Replacement of Renal Function by Dialysis*, 3rd ed. Netherlands, Kluwer Academic Publishers, 1989, pp. 144.
7. Clark WR: Hemodialyzer membranes and configurations: a historical perspective. *Semin Dial* 13: 309–311, 2000.
8. Freeman RB, Roushey G, Hegadus V, Pabico RC, Cestero R: Clinical implications of fluid mechanics in parallel flow plate diayzers. *Clin Nephrol* 2: 63–67, 1974.
9. Riede G: Development of the Lundia Pro dialyser. *Blood Purif* 4: 13–22, 1986.
10. Tuhy AR, Anderson EK, Jovanovic GN: Urea separation in flat-plate microchannel hemodialyzer; experiment and modeling. *Biomed Microdevices* 14: 595–602, 2012.
11. Twardowski ZJ: History of hemodialyzers' designs. *Hemodial Int* 12: 173–210, 2008.
12. Fissell WH, Dubnisheva A, Eldridge AN, Fleischman AJ, Zydney AL, Roy S: High-performance silicon nanopore hemofiltration membranes. *J Memb Sci* 326: 58–63, 2009.
13. Ahmadi M, Gorbet M, Yeow JT: *In vitro* clearance and hemocompatibility assessment of ultrathin nanoporous silicon membranes for hemodialysis applications using human whole blood. *Blood Purif* 35: 305–313, 2013.
14. Johnson DG, Khire TS, Lyubarskaya YL, *et al*: Ultrathin silicon membranes for wearable dialysis. *Adv Chronic Kidney Dis* 20: 508–515, 2013.
15. Kanani DM, Fissell WH, Roy S, Dubnisheva A, Fleischman A, Zydney AL: Permeability—selectivity analysis for ultrafiltration: effect of pore geometry. *J Memb Sci* 349: 405, 2010.
16. Muthusubramaniam L, Lowe R, Fissell WH, *et al*: Hemocompatibility of silicon-based substrates for biomedical implant applications. *Ann Biomed Eng* 39: 1296–1305, 2011.
17. Olorunsola OG, Kim SH, Chang R, et al: Imaging assessment of a portable hemodialysis device: detection of possible failure modes and monitoring of functional performance. *Med Instrum* 2: 2, 2014.
18. Rasband WS. Image J. Bethesda, Maryland, USA, U.S. National Institutes of Health. Available at: http://imagej.nih.gov/ij/. Accessed February 18, 2014.
19. Bankhead P. Analyzing fluorescence microscopy images with ImageJ. Available at: http://imagej.nih.gov/ij/docs/examples/. Accessed January 17, 2014.
20. Schneider CA, Rasband WS, Eliceiri KW: NIH Image to ImageJ: 25 years of image analysis. *Nat Methods* 9: 671–675, 2012.
21. Hemodialysis Adequacy 2006 Work Group. Clinical practice guidelines for hemodialysis adequacy, update 2006. *Am J Kidney Dis* 48 (Suppl 1):S2–S90, 2006.